Academia Journal of Environmetal Science 6(5): 113-120, May 2018

DOI: 10.15413/ajes.2018.0114 ISSN: ISSN 2315-778X ©2015 Academia Publishing





# Research Paper

# Seismo electric field fractal dimension for characterizing Shajara reservoirs of the Permo-Carboniferous Shajara Formation, Saudi Arabia

Accepted 8th May, 2018

#### **ABSTRACT**

The quality of a reservoir can be described in details by the application of seismo electric field fractal dimension. The objective of this research is to calculate fractal dimension from the relationship among seismo electric field, maximum seismo electric field and wetting phase saturation and to confirm it by the fractal dimension derived from the relationship among capillary pressure and wetting phase saturation. In this research, porosity was measured on real collected sandstone samples and permeability was calculated theoretically from capillary pressure profile measured by mercury intrusion techniques. Two equations for calculating the fractal dimensions were employed. The first one describes the functional relationship between wetting phase saturation, seismo electric field, maximum seismo electric field and fractal dimension. The second equation implies to the wetting phase saturation as a function of capillary pressure and the fractal dimension. Two procedures for obtaining the fractal dimension were also developed. The first procedure was done by plotting the logarithm of the ratio between seismo electric field and maximum seismo electric field versus logarithm wetting phase saturation. The slope of the first procedure = 3- Df (fractal dimension). The second procedure for obtaining the fractal dimension was completed by plotting the logarithm of capillary pressure versus the logarithm of wetting phase saturation. The slope of the second procedure = Df -3. On the basis of the obtained results of the constructed stratigraphic column and the acquired values of the fractal dimension, the sandstones of the Shajara reservoirs of the Shajara formation were divided into three units. The gained units from bottom to top are: Lower Shajara Seismo Electric Field Fractal Dimension Unit, Middle Shajara Seismo Electric Field Fractal dimension Unit and Upper Shajara Seismo Electric Field Fractal Dimension Unit. The results show similarity between seismo electric field fractal dimension and capillary pressure fractal dimension. It was also noted that samples with wide range of pore radius were characterized by high values of fractal dimension due to an increase in their connectivity and seismo electric field. In our case, and as conclusions the higher the fractal dimension, the higher the permeability and the better the shajara reservoir characteristics.

Khalid Elyas Mohamed Elameen Alkhidir

Department of Petroleum and Natural Gas Engineering, College of Engineering, King Saud University, Saudi Arabia.

E-mail: kalkhidir@ksu.edu.sa.

**Key words:** Shajara reservois, Shajara formation, seismo electric field fractal dimension.

### INTRODUCTION

Seismo electric effects related to electro kinetic potential, dielectric permitivity, pressure gradient, fluid viscosity, and

electric conductivty was first reported by Frenkel (1944). Capillary pressure follows the scaling law at low wetting

phase saturation as reported by Toledo et al. (1994) in Li and Williams (2007). Revil and Jardani (2010) reported seismo electric phenomenon by considering electro kinetic coupling coefficient as a function of effective charge density, permeability, fluid viscosity and electric conductivity.

Dukhin et al. (2010) reported that the magnitude of seismo electric current depends on porosity, pore size, zeta potential of the pore surfaces and elastic properties of the matrix. The tangent of the ratio of converted electic field to pressure is approximately in inverse proportion to permeability (Guan et al., 2012). Hu et al. (2012) studied the permeability inversion from seismoelectric log at low frequency and reported that, the tangent of the ratio among electric excitation intensity and pressure field is a function of porosity, fluid viscosity, frequency, tortuosity, fluid density and Dracy permeability.

Bordes et al. (2015) reportet on an decrease of seismo electric frequencies with increasing water content, while Jardani and Revil (2015) reported on an increase of seismo electric transfer function with increasing water saturation. Holzhauer et al. (2016) emphasized on the increase of dynamic seismo electric transfer function with decreasing fluid conductivity. The amplitude of seismo electric signal increases with increasing permeability which means that the seismo electric effects are directly related to the permeability and can be used to study the permeability of the reservoir was illustrated by Rong et al. (2016).

Seismo electric coupling is frequency dependent and decreases exponentially when frequency increases is demonstrated (Djuraev et al., 2017). Alkhidir (2017) reported on an increase of permeability with increasing pressure head and bubble pressure fractal dimension. Alkhidir (2018) also reported on an increase of geometric and arithmetic relaxtion tiome of induced polarization fractal dimension with permeability increase.

### **MATERIALS AND METHODS**

Porosity was measured on collected sandstone samples, while permeability was calculated from the measured capillary pressure by mercury intrusion techniques. Two procedures for obtaining the fractal dimension were also developed. The first procedure was done by plotting the logarithm of the ratio between seismo electric field and maximum seismo electric field versus logarithm wetting phase saturation. The slope of the first procedure was given as = 3- Df (fractal dimension), while the second procedure for obtaining the fractal dimension was completed by plotting the logarithm of capillary pressure versus the logarithm of wetting phase saturation. The slope of the second procedure is given as= Df -3. The seismo electric field can be scaled as:

$$Sw = \left[\frac{E^{\left[\frac{1}{3}\right]}}{E_{\max}^{\left[\frac{1}{3}\right]}}\right]^{\left[3-Df\right]} \tag{1}$$

Where  $S_w$  the water saturation, E the seismo electric field in volt / meter,  $E_{max}$ , the maximum seismo electric field in volt / meter, and Df the fractal dimension.

Equation 1 can be proofed from:

$$\mathbf{E} = \left[ \frac{\mathbf{E}\mathbf{f} * \mathbf{\zeta} * \mathbf{\rho} \mathbf{f} * \ddot{\mathbf{U}}}{\mathbf{\eta} * \mathbf{\sigma} \mathbf{f}} \right] \tag{2}$$

Where E is the seismo electric field in volt / meter,  $\epsilon f$  dielectric permittivity of the fluid,  $\zeta$  the zeta potential in volt,  $\rho f$  density of the fluid in kilogram / cubic meter,  $\ddot{\upsilon}$  the seismo electric acceleration in meter / second square,  $\eta$  the fluid viscosity in pascal second, and  $\sigma f$  the fluid conductivity in Siemens /meter.

But, 
$$\frac{\varepsilon f * \zeta}{\eta * \sigma f} = C_s$$
 (3)

Where  $C_S$ , the streaming potential coefficient in volt / pascal.

Insert Equation 3 into 2, we have:

$$\mathbf{E} = \mathbf{C}_{s} * \mathbf{\rho} \mathbf{f} * \ddot{\mathbf{U}} \tag{4}$$

The streaming potential can be scaled as:

$$\mathbf{C_S} = \frac{\mathbf{V}}{\mathbf{Q}} \tag{5}$$

Where V is the volume in cubic meter, Q the electric charge in coulomb.

Insert Equation 5 into Equation 4, we have:

$$\mathbf{E} = \left[ \frac{\mathbf{V} * \mathbf{\rho} \mathbf{f} * \ddot{\mathbf{U}}}{\mathbf{Q}} \right] \tag{6}$$

The volume V can be scaled as:

$$V = \frac{4}{3} * 3.14 * r^3$$
 (7)

Where r the pore radius in meter.

Insert Equation 7 into Equation 6, it becomes:

$$E = \left[ \frac{4 * 3.14 * r^{3} * \rho f * \ddot{\textbf{U}}}{3 * Q} \right] \tag{8}$$

The maximum pore radius  $r_{max}$  can be scaled as:

$$E_{max} = \left[ \frac{4 * 3.14 * r_{max}^{3} * \rho f * \ddot{U}}{3 * Q} \right]$$
(9)

Divide Equation 8 by Equation 9, we have:

$$\left[\frac{E}{E_{max}}\right] = \left[\frac{\frac{4*3.14*r^3*\rho f*\ddot{\upsilon}}{3*Q}}{\frac{4*3.14*r_{max}^3*\rho f*\ddot{\upsilon}}{3*Q}}\right]$$
(10)

Equation 10 after simplification will become:

$$\left[\frac{E}{E_{max}}\right] = \left[\frac{r^3}{r_{max}^3}\right] \tag{11}$$

Take the third root of Equation 11:

$$\sqrt[3]{\left[\frac{\mathbf{E}}{\mathbf{E}_{\max}}\right]} = \sqrt[3]{\left[\frac{\mathbf{r}^3}{\mathbf{r}_{\max}^3}\right]} \tag{12}$$

Equation 12 after simplification and addition of logarithm will become:

$$log[E^{1/3}/E_{max}^{1/3}] = log[r/r_{max}]$$
 (13)

But, 
$$Log[r/r_{max}] = logS_w/[3-Df]$$
 (14)

Insert Equation 14 into Equation 13, it becomes:

$$\log S_{w}/[3-Df] = \log[E^{1/3}/E_{max}^{1/3}]$$
 (15)

Equation 15 after log removal will become:

$$S_{W} = \left[\frac{E^{\left[\frac{1}{3}\right]}}{E^{\left[\frac{1}{3}\right]}_{max}}\right]^{[3-Df]} \tag{16}$$

Equation 16 which is the proof of Equation 1 relates to water saturation, seismo electric field, maximum seismo electric field and the fractal dimension.

The capillary pressure can be scaled as:

$$\log S_{w} = (Df-3)* \log p_{c} + constant$$
 (17)

Where Sw is the water saturation, Pc: the capillary pressure and Df: the fractal dimension.

#### **RESULTS AND DICNUSSION**

Based on field observation the Shajara Reservoirs of the Permo-Carboniferous Shajara Formation were divided into three units as described (Figure 1). These units from bottom to top are: Lower, Middle, and Upper Shajara Reservoir. Their acquired results of the seismo electric fractal dimension and capillary pressure fractal dimension are displayed in Table 1.

Based on the attained results it was found that the seismo electric fractal dimension is equal to the capillary pressure fractal dimension. The maximum value of the fractal dimension was found to be 2.7872 assigned to sample SJ13 from the Upper Shajara Reservoir as verified in Table 1. Whereas the minimum value of the fractal dimension 2.4379 was reported from sample SJ3 from the Lower Shajara reservoir as displayed in Table 1. The seismo electric fractal dimension and capillary pressure fractal dimension were observed to increase with increasing permeability owing to the possibility of having interconnected channels (Table 1).

The Lower Shajara reservoir was denoted by six sandstone samples (Figure 1), four of which label as SJ1, SJ2, SJ3 and SJ4 as confirmed in Table 1 were selected for capillary measurements. Their positive slopes of the first procedure (log of the ratio of seismo electric field to maximum seismo electric field versus log wetting phase saturation) and negative slopes of the second procedure (log capillary pressure versus log wetting phase saturation are delineated (Figures 2, 3, 4 and 5) and (Table 1). Table 1 shows their seismo electric field fractal dimension and capillary pressure fractal dimension values. As we proceed from sample SI2 to SI3 a pronounced reduction in permeability due to compaction was reported from 1955 md to 56 md which reflects decrease in seismo electric field fractal dimension from 2.7748 to 2.4379 as specified in Table 1. In addition, an increase in grain size and permeability was verified from sample SJ4 whose seismo electric field fractal dimension and capillary pressure fractal dimension was found to be 2.6843 (Table 1).

In contrast, Figure 1 shows the Middle Shajara reservoir is separated from the Lower Shajara reservoir by an unconformity surface. It was designated by three samples and four sandstone samples (Figure 1), three of which namely SJ7, SJ8, and SJ9 as illustrated in Table 1 and Figure 1 were preferred to perform capillary pressure measurements. Their positive slopes of the first procedure and negative slopes of the second procedure are shown in Figures 6, 7 and 8 and Table 1. Additionally, Table 1 shows similarities in their seismo electric field fractal dimensions and capillary pressure fractal dimensions. Their fractal dimension values are higher than those of samples SJ3 and SJ4 from the Lower Shajara Reservoir due to an increase in their permeability (Table 1).

On the other hand, Figure 1 shows the Upper Shajara reservoir separated from the Middle Shajara reservoir by

AGE	Fm.	Mbr.	unit	LITHO- LOGY	DESCRIPTION		
Late	Khuff Formation	Huqayl			Limestone : Cream, dense, burrowed, thickness 6.56		
reman	rotmation	Member		~~~	Sub-Khuff unconformity.		
Late Carboniferous - Permian	Shajara Formation	Upper Shajara Member	Upper Shajara mudstone		Mudstone : Yellow, thickness 17.7		
			Upper Stajar Reservoir	SJ13▲ SJ12▲	Sandstone: Light brown, cross-beded, coarse-grained, poorly sorted, porous, friable, thickness 6.5'		
					Sandstone: Yellow, medium-grained, very coarse-grained,		
					poorly, moderately sorted, porous, friable, thickness 13.1°		
		Middle Shajara Member	Middle Shajara mudstone	SJII	Mudstone: Yellow-green, thickness 11.8'  Mudstone: Yellow, thickness 1.3'  Mudstone: Brown, thickness 4.5'		
			Middle Shajara Reservoir	SJ10▲	Sandstone: Light brown, medium-grained, moderately sorted, porous, friable, thickness 3.6'		
				SJ9▲ SJ8▲ SJ7▲	Sandstone: Yellow, medium-grained, moderately well sorted, porous, friable, thickness 0.9'  Sandstone: Red, coarse-grained, medium-grained, moderately well sorted, porous, friable, thickness 13.4'		
		Lower Shajara Member	Lower Shajara Reservoir	SJ5	Sandstone: White with yellow spots, fine-grained., hard, thickness 2.6' Sandstone: Limonite, thickness 1.3'		
				SJ4▲	Sandstone: White, coarse-grained, very poorly sorted, thickness 4.5°		
				SJ3A~~	Sandstone: White-pink, poorly sorted, thickness 1.6'		
				SJI▲	Sandstone: Yellow, medium-grained, well sorted, porous, friable, thickness 3.9'		
					Sandstone: Red, medium-grained, moderately well sorted, porous, friable, thickness 11.8'		
Carlo				~~~	Sub-Unayzah unconformity.		
Early evonian	Tawil Formation			selled to the	Sandstone : White, fine-grained. SJ1 ▲ Samples Collecti		

**Figure 1:** Surface type section of the Shajara Reservoirs of the permo-Carboniferous Shajara Formation, Saudi Arabia latitude 26 52 17.4 longitude 43 36 18.

**Table 1:** Petrophysical model showing the three Shajara reservoirs of their corresponding values of seismo electric fractal dimension and capillary pressure fractal dimension.

Reservoir	Sample	Φ %	K (md)	Postive slope of the first procedure (Slope =3-Df)	negative slope of the second procedure (Slope=Df-3)	Seismo electric field fractal dimension	Pressure fractal dimension
	SJ13	25	973	0.2128	-0.2128	2.7872	2.7872
Upper Shajara reservoir	SJ12	28	1440	0.2141	-0.2141	2.7859	2.7859
reservon	SJ11	36	1197	0.2414	-0.2414	2.7586	2.7586
	SJ9	31	1394	0.2214	-0.2214	2.7786	2.7786
Middle Shajara Reservoir	SJ8	32	1344	0.2248	-0.2248	2.7752	2.7752
Reservoir	SJ7	35	1472	0.2317	-0.2317	2.7683	2.7683
	SJ4	30	176	0.3157	-0.3157	2.6843	2.6843
Lower Shajara	SJ3	34	56	0.5621	-0.5621	2.4379	2.4379
Reservoir	SJ2	35	1955	0.2252	-0.2252	2.7748	2.7748
	SJ1	29	1680	0.2141	-0.2141	2.7859	2.7859

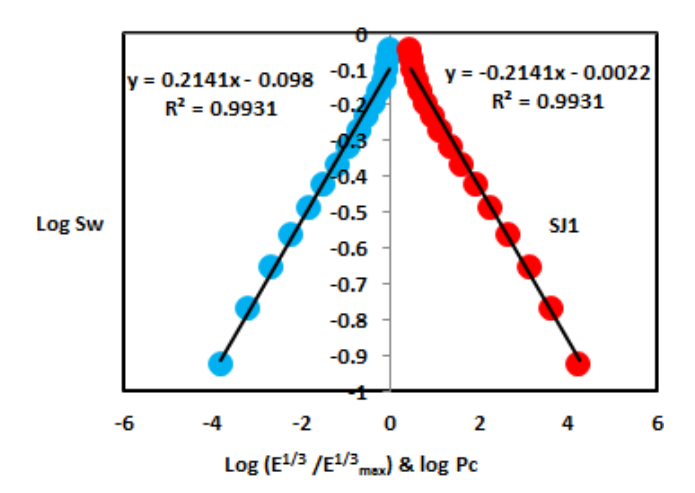


**Figure 2:** Log ( $E^{1/3}$  /  $E^{1/3}_{max}$ ) & log pc versus log Sw for sample SJ.

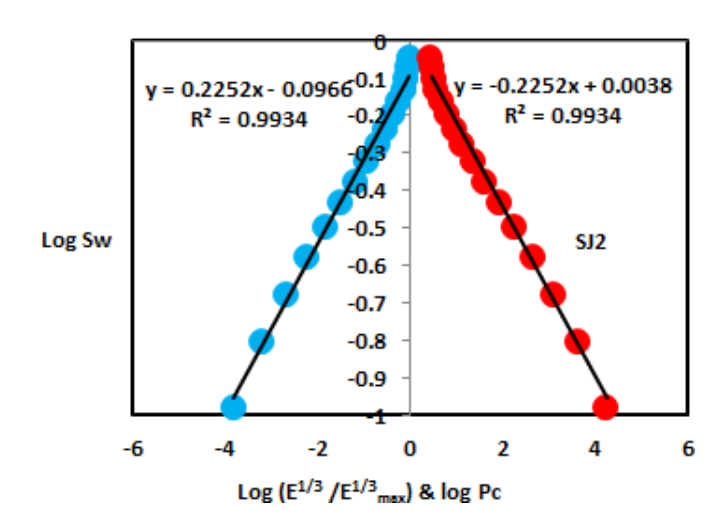


**Figure 3:** Log  $(E^{1/3} / E^{1/3}_{max})$  and log pc versus log Sw for sample SJ2.

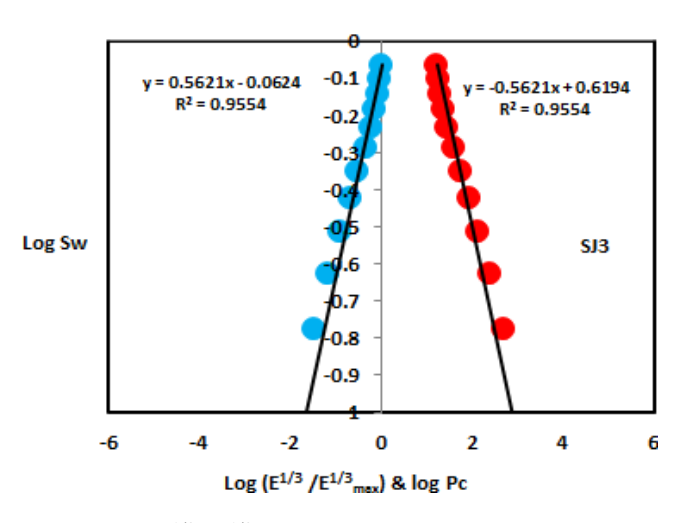


**Figure 4:** Log  $(E^{1/3} / E^{1/3}_{max})$  & log pc versus log Sw for sample SJ3.

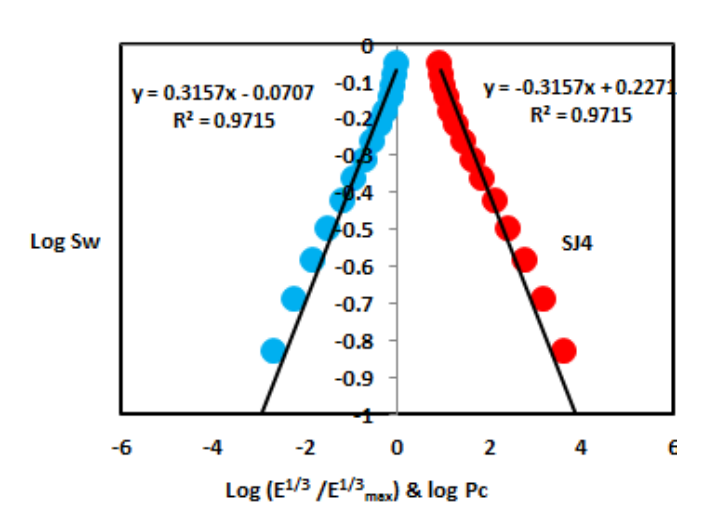
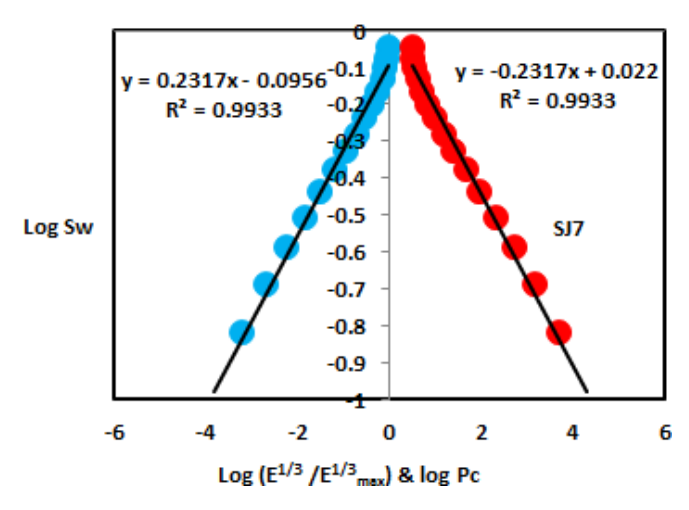
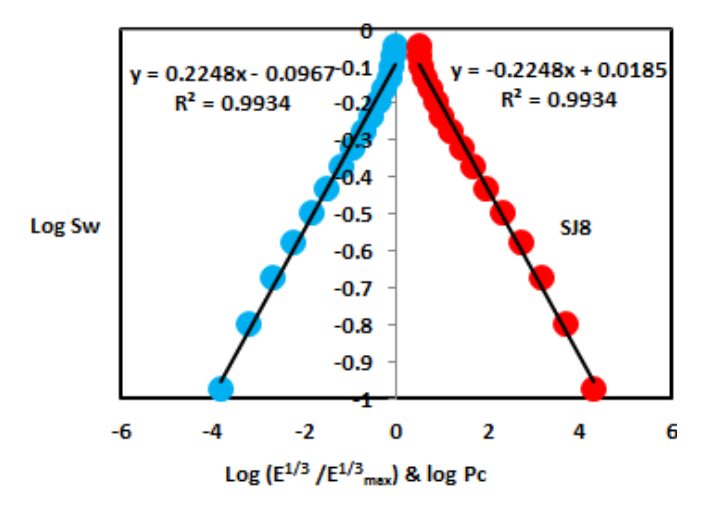


Figure 5: Log (E  $^{1/3}$  / E  $^{1/3} \text{max}$  ) & log pc versus log Sw for sample SJ4.



**Figure 6:** Log  $(E^{1/3} / E^{1/3}_{max})$  & log pc versus log Sw for sample SJ7.



**Figure 7:** Log  $(E^{1/3} / E^{1/3}_{max})$  & log pc versus log Sw for sample SJ8.

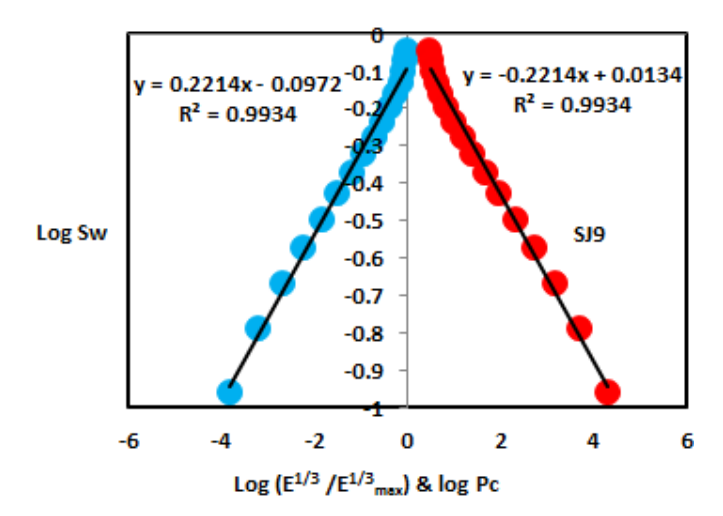


**Figure 8:** Log  $(E^{1/3} / E^{1/3}_{max})$  & log pc versus log Sw for sample SJ9.

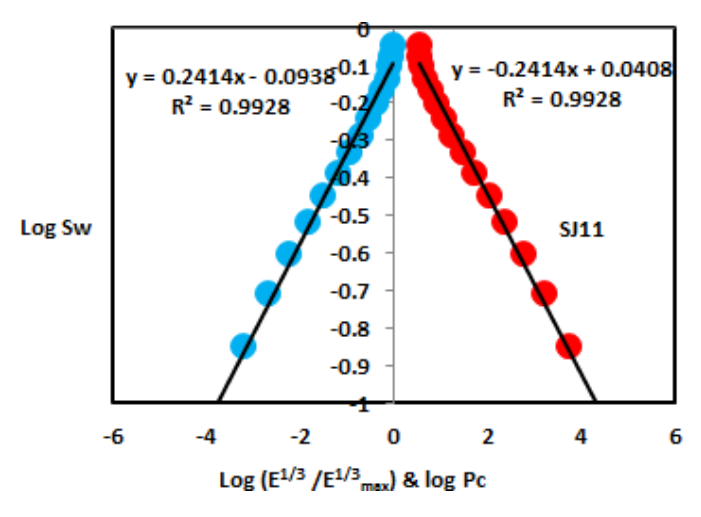


**Figure 9:** Log ( $E^{1/3}$  /  $E^{1/3}_{max}$ ) & log pc versus log Sw for sample SJ11.

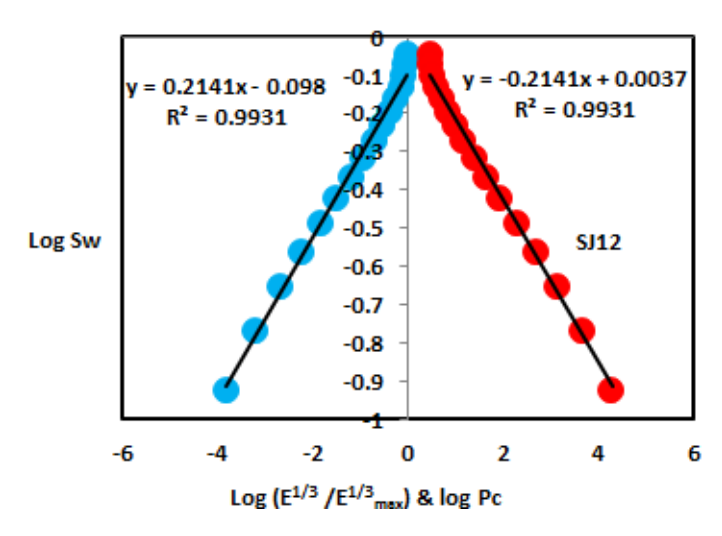


**Figure 10:** Log  $(E^{1/3} / E^{1/3}_{max})$  & log pc versus log Sw for sample SJ12.

yellow green mudstone. It is defined by three samples so called SJ11, SJ12 and SJ13 (Table 1). Their positive slopes of the first procedure and negative slopes of the second procedure are displayed in Figures 9, 10 and 11 and Table 1. Moreover, their seismo electric field fractal dimension and capillary pressure fractal dimension are also higher than those of sample SJ3 and SJ4 from the Lower Shajara Reservoir due to an increase in their permeability (Table 1).

Overall, a plot of slopes of the first procedure versus the slopes of the second procedure delineates three permeable zones as presented in Figure 12. These reservoir zones were also proofed by seismo electric field fractal dimension versus capillary pressure fractal dimension (Figure 13). Such variation in fractal dimension can account for heterogeneity which is a key parameter in reservoir quality assessment.

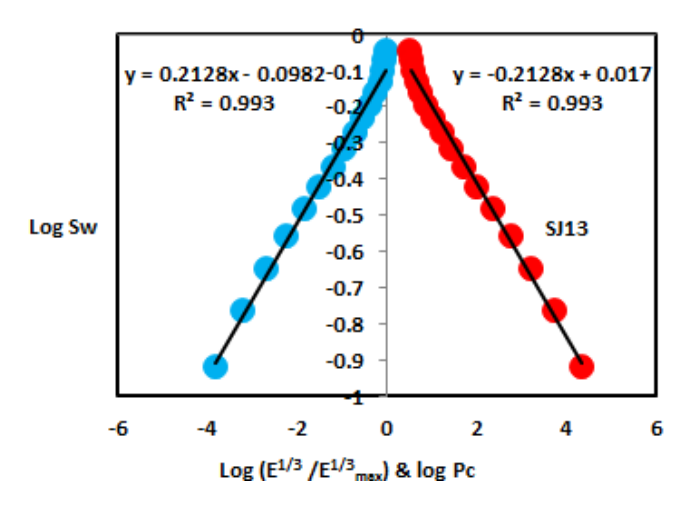


**Figure 11:** Log  $(E^{1/3} / E^{1/3}_{max})$  & log pc versus log Sw for sample SI13.

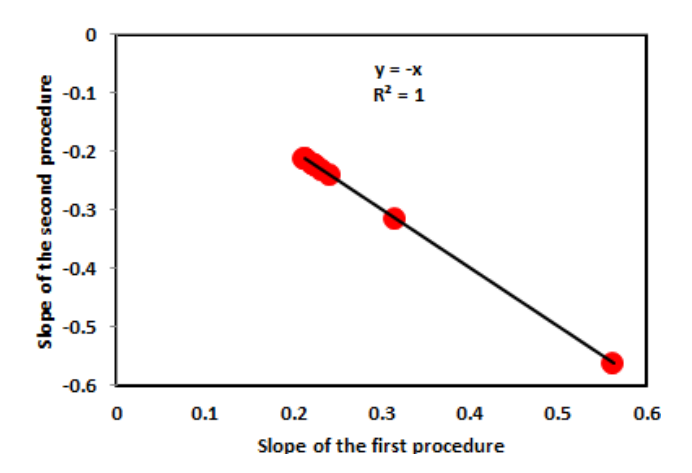


**Figure 12:** Slope of the first procedure versus the slope of the second procedure.

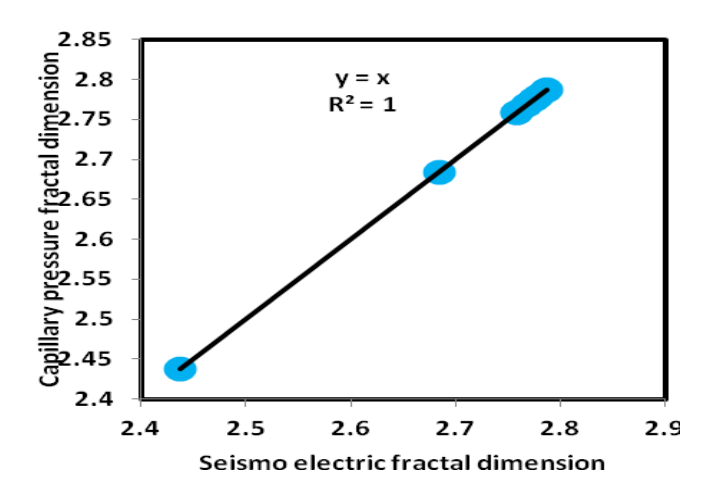


**Figure 13:** Seismo electric fractal dimension versus capillary pressure fractal dimension.

#### **Conclusions**

The following conclusions can be drawn from this study:

- 1) The sandstones of the Shajara Reservoirs of the permo-Carboniferous Shajara formation were divided into three units based on seismo electric field fractal dimension;
- 2) The Units from bottom to top are: Lower Shajara seismo electric Field Fractal dimension Unit, Middle Shajara Seismo Electric Field Fractal Dimension Unit, and Upper Shajara Seismo-electric Fractal Dimension Unit;
- 3) These units were also proved by capillary pressure fractal dimension;
- 4) The fractal dimension was found to increase with increasing grain size and permeability.

#### **ACKNOWLEDGMENTS**

The author would to thank King Saud University, College of Engineering, Department of Petroleum and Natural Gas Engineering, Department of Chemical Engineering, Research Centre at College of Engineering, and King Abdullah, Institute for Research and Consulting Studies for their supports.

# REFERENCES

Alkhidir KEME (2017). Pressure head fractal dimension for characterizing Shajara Reservoirs of the Shajara Formation of the Permo-Carboniferous Unayzah Group, Saudi Arabia. Arch. Pet. Environ. Biotechnol. 2: 1-7.

Alkhidir KEME (2018). Geometric relaxation time of induced polarization fractal dimension for characterizing Shajara Reservoirs of the Shajara Formation of the Permo-Carboniferous Unayzah Group, Saudi Arabia. SF J. Pet. 2(1): 1-6.

Borde C, S'en'echal P, Barri'ere J, Brito D, Normandin E, Jougnot D (2015). Impact of water saturation on seismoelectric transfer functions: A laboratory study of co-seismic phenomenon. Geophys. J. Int. 200(3): 1317-1335.

Djuraev U, Jufar S, Vasant P (2017). Numerical Study of frequency-dependent seismoelectric coupling in partially-saturated porous media. MATEC Web Conf. 87(02001): 6.

Dukhin A, Goetz P, Thommes M (2010). Seismoelectric effect: A nonisochoric streaming current. 1 Experiment. J. Colloid Interface Sci. 345(2): 547-553.

Frenkel J (1944). On the theory of seismic and seismoelectric phenomena in a moist soil. J. Phys. 3(4): 230-241.

Guan W, Hu H, Wang Z (2012). Permeability inversion from low-frequency seismoelectric logs in fluid-saturated porous formations. Geophys. Prospect. 61(1): 120-133.

Holzhauer J, Brito D, Bordes C, Brun Y, Guatarbes B (2016). Experimental quantification of the seismoelectric transfer function and its dependence on conductivity and saturation in loose sand. Geophys. Prospect. 65(4): 1097-1120.

Hu H, Guan W, Zhao W (2012). Theoretical studies of permeability inversion from seismoelectric logs. Geophysical Research Abstracts. 14: EGU2012-6725-1, 2012 EGU General Assembly 2012.

Jardani A, Revi A (2015). Seismoelectric couplings in a poroelastic material containing two immiscible fluid phases. Geophys. J. Int. 202(2): 850-870.

Li K, Williams W (2007). Determination of capillary pressure function from resistivity data. Transp. Porous Media. 67(1): 1-15.

Revil A, Jardani A (2010). Seismoelectric response of heavy oil reservoirs: theory and numerical modelling. Geophys. J. Int. 180(2): 781-797. Rong P, Xing W, Rang D,Bo D, Chun L (2016). Experimental research on seismoelectric effectsin sandstone. Appl. Geophys. 13(3): 425-436.

# Cite this article as:

Alkhidir KEME (2018). Seismo electric field fractal dimension for characterizing Shajara reservoirs of the Permo-Carboniferous Shajara Formation, Saudi Arabia. Acad. J. Environ. Sci. 6(5): 113-120.

# Submit your manuscript at:

http://www.academiapublishing.org/ajes